INORGANIC CHEMISTRY
FRONTIERS

RESEARCH ARTICLE

Cite this: DOI: 10.1039/c8qi00469b

Solvent-induced framework-interpenetration isomers of Cu MOFs for efficient light hydrocarbon separation†

Yutong Wang, ‡[a] Weidong Fan,‡[a] Xia Wang,[a] Yinfeng Han,*[a,b] Liangliang Zhang, [a] Di Liu, [c] Fangna Dai *[a] and Daofeng Sun [a]

Received 22nd May 2018,
Accepted 28th June 2018
DOI: 10.1039/c8qi00469b
rsc.li/frontiers-inorganic

By tuning interpenetrated and non-interpenetrated frameworks, a pair of Cu-paddlewheel framework-interpenetration isomers (**UPC-34**, $[Cu_3(L)_2(H_2O)_3]\cdot 2DMF\cdot 3EtOH\cdot 3H_2O$ and **UPC-35**, $[Cu_3(L)_2(H_2O)_3]\cdot 2DMF\cdot 2Diox\cdot 3H_2O$) based on a tripodal ligand (H_3**L** = 4,4′-((5-carboxy-1,3-phenylene)bis(ethyne-2,1-diyl)) dibenzoic acid) has been synthesized and characterized. The interpenetrated framework (**UPC-35**) is more stable than the non-interpenetrated one (**UPC-34**). Due to the 2-fold interpenetration, **UPC-35** has a pore size distribution of ~4.5 Å, which is close to the kinetic diameters of light hydrocarbons (C_1–C_3), and thus exhibits high gas-uptake capacities for C_3H_6 and C_3H_8. Furthermore, **UPC-35** is an effective adsorbent for the selective separation of $C_3/C_2/C_1$ light hydrocarbons.

Petroleum cracking is an important and complicated chemical process, its gas by-products mainly include hydrogen, methane, ethane, ethylene, acetylene propane, propylene, *etc*.[1] As the main component of natural gas and shale gas, methane (C_1) is a clean energy source that can be used as civil gas and automobile fuel. Acetylene, ethylene, propylene and other light hydrocarbons (C_2–C_3) are basic raw materials for industry, for example, in the production of polyethylene and polypropylene.[2] It is necessary to obtain high purity light hydrocarbon components for efficient utilization. Therefore, the separation of light hydrocarbons ($C_3/C_2/C_1$) is of great significance.[3]

Traditional technologies used for $C_3/C_2/C_1$ separation include cryogenic processes, expander processes, middle low temperature oil absorption processes, *etc*., which have high energy consumption.[4] Compared with these traditional separation technologies, adsorption separation methods can be realized at a normal temperature and pressure, and the cost and energy consumption are relatively low.[5] However, due to the limited surface areas and uncontrollable structures of traditional adsorbents, such as zeolites, molecular sieves, and activated carbon, it is difficult to achieve effective light hydrocarbon separation.[6] Therefore, developing new effective adsorbents is essential for the separation of light hydrocarbons.[7]

As a new class of porous crystalline materials, metal–organic frameworks (MOFs), which are assembled from metal ions/clusters and organic linkers, have attracted wide research interest for gas storage and separation.[8] There are lots of reports on the separation of H_2/N_2 and H_2/CO_2 by MOFs,[9] while reports are less common for light hydrocarbons, partly because of a mismatch between the pore sizes of MOFs and the kinetic diameters of light hydrocarbons.[10] Recently, Eddaoudi *et al.* achieved the selective separation of propylene and propane by controlling the pore size distribution of ~4.0 Å;[11] Zhang *et al.* realized efficient separation of C_2H_4/C_2H_6 (99.95%) by adding hydrogen bond acceptors and dipole repulsive groups in the pores;[12] Chen *et al.* designed and synthesized tetrahedral interpenetrating MOF materials for separating acetylene and methane with high selectivity, and the separation selectivity was 35.[13] Usually, there are three strategies for light hydrocarbon separation by MOFs: (1) introducing modified functional groups to increase the binding force between host MOFs and guest gases; (2) designing flexible or breathing structures and pores for the passage of specific gases; (3) controlling structures to limit pore sizes for matching to the light hydrocarbons' kinetic diameters, for example, by interpenetration. It should be pointed out that although the interpenetration phenomenon can be utilized for preparing MOFs with specific pore sizes, interpenetration can also

[a]*College of Science, China University of Petroleum (East China), Qingdao, Shandong 266580, P. R. China. E-mail: fndai@upc.edu.cn, han@tsu.edu.cn*
[b]*Department of Chemistry and Chemical Engineering, Taishan University, Tai'an, Shandong 271021, P. R. China*
[c]*College of Chemical and Environmental Engineering, Shandong University of Science and Technology, Qingdao, Shandong, 266590, P. R. China*

†Electronic supplementary information (ESI) available: Synthesis of H_3**L**, **UPC-34** and **UPC-35**, crystal data, TGA curves, IR patterns, and C_2H_6/CH_4, C_2H_4/CH_4, C_2H_2/CH_4, C_3H_8/CH_4 and C_3H_6/CH_4 selectivities at 273 K and 298 K. CCDC 1835836 and 1835837. For ESI and crystallographic data in CIF or other electronic formats see DOI: 10.1039/c8qi00469b

‡These authors contributed equally to this work.

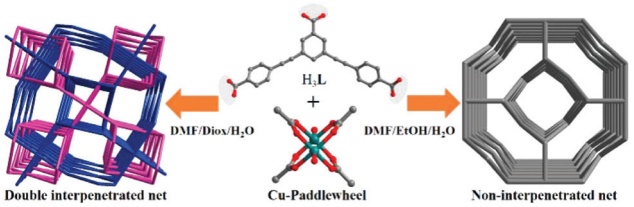

Scheme 1 A schematic illustration of the solvent-induced framework-interpenetration isomer.

reduce surface areas.[14] Therefore, it is important to regulate the interpenetrated framework while simultaneously retaining the high light hydrocarbon adsorption ability (Scheme 1).[15]

In this communication, we report a pair of solvent-induced framework-interpenetration isomers of Cu MOFs (**UPC-34**, $[Cu_3(L)_2(H_2O)_3]\cdot 2DMF\cdot 3EtOH\cdot 3H_2O$ and **UPC-35**, $[Cu_3(L)_2(H_2O)_3]\cdot 2DMF\cdot 2Diox\cdot 3H_2O$) based on a tripodal H_3**L** ligand. The non-interpenetrated isomer of **UPC-34** can not retain its framework upon the removal of guest molecules in the channels. In contrast, the interpenetrated framework, **UPC-35**, exhibits permanent porosity with a BET surface area of 1087 $m^2\ g^{-1}$. Furthermore, **UPC-35** possesses high C_3H_6 and C_3H_8 uptake, and also exhibits efficient separation of light hydrocarbons.

Needle crystals of **UPC-34** and block crystals of **UPC-35** were obtained by the solvothermal reaction of H_3**L** and $Cu(NO_3)_2\cdot 2.5H_2O$ at 75 °C for two days. It should be pointed out that the formation of **UPC-34** and **UPC-35** is controlled by the solvents, *N*,*N*-dimethylformamide (DMF)/ethanol (EtOH)/H_2O (5 : 2 : 1, v/v/v) for **UPC-34** and DMF/1,4-dioxane (Diox)/H_2O (5 : 2 : 1, v/v/v) for **UPC-35**. The slight change in one of the components of the mixed solvent (Diox *vs.* EtOH) can fine tune the interpenetration and non-interpenetration, and allow the formation of the framework-interpenetration isomer, which was seldom reported previously. Single crystal X-ray diffraction reveals that **UPC-34** crystallizes in the tetragonal system with the space group of *I*4/*mcm*, whereas **UPC-35** crystallizes in the tetragonal system with the space group of *I*4/*m*. The crystallographic data are summarized in Table S1† and selected bond lengths and bond angles are listed in Tables S2–5.†

As shown in Fig. 1a, **UPC-34** exhibits a non-interpenetrating framework with a ***fjh*** net. Each pair of Cu(II) ions is bridged by four L^{3-} ligands to form a typical dinuclear Cu paddlewheel unit ($Cu_2(COO)_4$ SBU) (Fig. S1a and S1b, ESI†). In the crystal structure of **UPC-34**, four L^{3-} ligands link four $Cu_2(COO)_4$ SBUs to generate a small square frame, which is embedded in a large octagonal frame formed by eight L^{3-} ligands and eight $Cu_2(COO)_4$ SBUs. The dimensions of the channels are 14.3 × 16.0 $Å^2$ along the *c*-axis (Fig. S3b, ESI†). A large amount of solvates reside in the channels. After removal of the guest solvents, a total solvent accessible volume of 84.5% (32 435.0 $Å^3$ out of the 38 378.0 $Å^3$ unit cell volume) was calculated based on the PLATON/VOID routine.

UPC-35 possesses a 2-fold interpenetrating framework with a ***pto*** net, based on the $Cu_2(COO)_4$ SBUs similar to that of

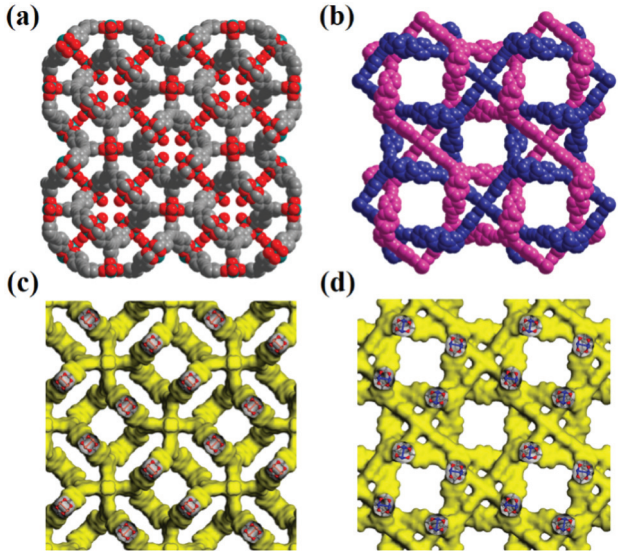

Fig. 1 (a) The 3D open framework of **UPC-34**; (b) the 2-fold interpenetrating framework of **UPC-35**; (c) and (d) the 3D structures of **UPC-34** and **UPC-35** with corrugated channels, respectively (the H atoms are omitted for clarity).

UPC-34. Each $Cu_2(COO)_4$ SBU attaches to four L^{3-} ligands, and each ligand connects three $Cu_2(COO)_4$ SBUs to generate an open framework with 3D channels (Fig. 1b and S3b, ESI†). The dimensions of the channels are 31.0 × 13.6 $Å^2$ and 12.6 × 12.3 $Å^2$ along the [001] direction in each interpenetrated net (Fig. S3b, ESI†). Due to the large channels, two such nets interpenetrate each other to provide a 3D interpenetrated framework, further stabilizing the whole framework. Despite the interpenetration, **UPC-35** is still porous with the dimensions of the channels being 7.1 × 7.1 $Å^2$ (Fig. S3b, ESI†). As shown in Fig. S2,† the difference between **UPC-34** and **UPC-35** is mainly the twist angle between the edge benzene ring and the center benzene ring. With a change of the twist angle, the network structure and the topology of the complexes changed significantly. After removal of the guest solvents, the total solvent accessible volume is 63.7% (12 666.0 $Å^3$ out of the 19 888.0 $Å^3$ unit cell volume), which is significantly lower than that of **UPC-34**.

The establishment of permanent porosity is an important goal in MOF research.[16] Unfortunately, **UPC-34** cannot retain its framework after the removal of the guest solvates in the channels, due to the larger pore size. In contrast, the active phase of **UPC-35** is highly crystalline, and can retain its framework after the removal of the solvates (Fig. S5, ESI†). **UPC-35** shows a type I N_2 adsorption isotherm at 77 K, suggesting permanent micro-porosity (Fig. 2). The N_2 gas uptake is 373 $cm^3\ g^{-1}$ at 77 K and 1 bar. The pore volume calculated is 0.58 $cm^3\ g^{-1}$, which is smaller than the theoretical one (0.70 $cm^3\ g^{-1}$) owing to structural contractions during activation. The Brunauer–Emmett–Teller (BET) and Langmuir surface areas calculated are 1087 and 1578 $m^2\ g^{-1}$, respectively.

Considering the small pore sizes and intrinsic permanent porosity of **UPC-35**, we have investigated its potential appli-

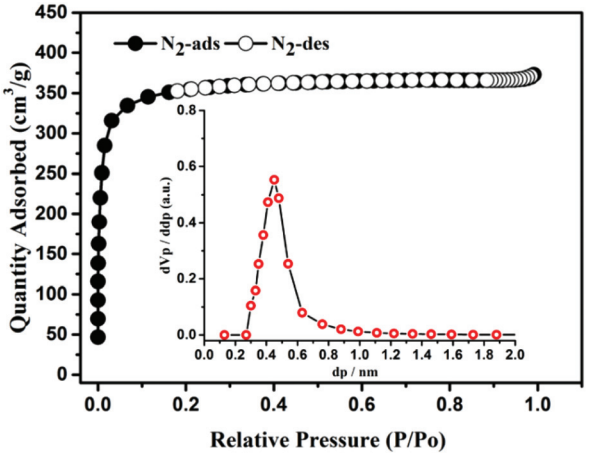

Fig. 2 The N_2 adsorption isotherm at 77 K and pore size distribution of **UPC-35**.

cation for light hydrocarbon (CH_4, C_2H_2, C_2H_4, C_2H_6, C_3H_6, and C_3H_8) adsorption and separation. Single component gas adsorption isotherms of **UPC-35** for various light hydrocarbons were performed at both 273 K and 298 K. As expected, **UPC-35** exhibits high uptakes of C_3H_8 (128.6 $cm^3\ g^{-1}$), C_3H_6 (138.1 $cm^3\ g^{-1}$), C_2H_6 (70.1 $cm^3\ g^{-1}$), C_2H_4 (56.4 $cm^3\ g^{-1}$), and C_2H_2 (72.5 $cm^3\ g^{-1}$), but a relatively low uptake of CH_4 (11.0 $cm^3\ g^{-1}$) at 273 K and 1 bar (Fig. 3a). It should be noted that the adsorption capacities of **UPC-35** for C_3H_8 (111.3 $cm^3\ g^{-1}$), C_3H_6 (118.3 $cm^3\ g^{-1}$), C_2H_6 (40.8 $cm^3\ g^{-1}$), C_2H_4 (35.9 $cm^3\ g^{-1}$), C_2H_2 (44.4 $cm^3\ g^{-1}$), and CH_4 (4.8 $cm^3\ g^{-1}$) can still be achieved at 298 K and 1 bar (Fig. 3b).[17] It is known that the magnitude of the heat of adsorption reveals the affinity of the pore surface toward adsorbents, which plays a significant part in determining the adsorptive selectivity. To evaluate the affinity of such light hydrocarbons in **UPC-35**, the heats of adsorption are calculated based on the Clausius–Clapeyron equation.[10b] The adsorption enthalpies (Q_{st}) for CH_4, C_2H_2, C_2H_4, C_2H_6, C_3H_6, and C_3H_8 are 18.4 kJ mol^{-1}, 22.7 kJ mol^{-1}, 18.4 kJ mol^{-1}, 22.7 kJ mol^{-1}, 24.5 kJ mol^{-1}, and 29.9 kJ mol^{-1} at zero coverage, respectively (Fig. 3c).

The C_3 light hydrocarbons with higher heats of adsorption may have stronger affinities for the skeleton, which indicates that these gases will be preferentially adsorbed on **UPC-35**. Thus, it may have a higher selectivity for C_3 light hydrocarbons compared to CH_4. Therefore, the potential for separation of CH_4 from C_3 light hydrocarbons has been appraised by ideal solution adsorbed theory (IAST) for binary equimolar components (Fig. 3d). At 1 bar and 273 K, the selectivities of C_3H_8 and C_3H_6 to CH_4 are 121.6 and 159.5, which are higher than the selectivities of C_2H_2, C_2H_4, and C_2H_6 to CH_4 which are 12.1, 8.5, and 11.2, respectively. It should be noted that these values are lower than in FJI-C4 (293.4 for C_3H_8/CH_4),[18] but substantially higher than in **UPC-21** (75 for C_3H_6/CH_4 and 67 for C_3H_8/CH_4),[19] and FJI-C1 (78.7 for C_3H_8/CH_4).[20] At 1 bar and 298 K, the selectivities of C_3H_8 and C_3H_6 to CH_4 are 87.6 and 86.9, which are higher than the selectivities of C_2H_2, C_2H_4, and C_2H_6 to CH_4 which are 13.1, 10.4, and 11.5, respectively. These results indicate that **UPC-35** is a prospective adsorbent for the effective separation of CH_4 from C_3 light hydrocarbons at room temperature. The high adsorption selectivity of C_3/C_1 could be attributed to the narrow

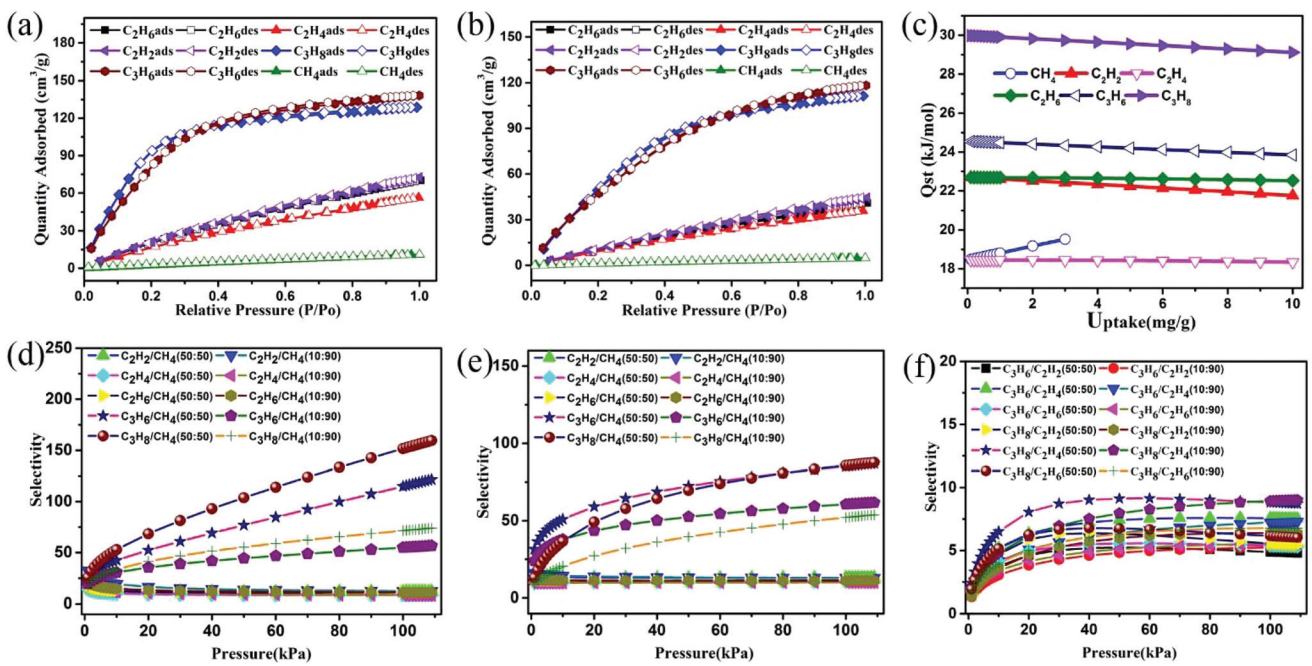

Fig. 3 (a) and (b) The CH_4, C_2H_6, C_2H_4, C_2H_2, C_3H_8 and C_3H_6 adsorption isotherms at 273 K and 298 K for **UPC-35**; (c) the Q_{st}; (d) and (e) the C_2H_6/CH_4, C_2H_4/CH_4, C_2H_2/CH_4, C_3H_8/CH_4 and C_3H_6/CH_4 selectivities at 273 K and 298 K, calculated by the IAST method (V/V: 50/50 and 10/90); (f) the C_3H_6/C_2H_2, C_3H_6/C_2H_4 and C_3H_6/C_2H_6 selectivities at 273 K, calculated by the IAST method (V/V: 50/50 and 10/90).

Table 1 A comparison of different materials for the adsorption of light hydrocarbons

Gas	CH_4		C_2H_2		C_2H_4		C_2H_6		C_3H_6		C_3H_8		
T [K]	273	298	273	298	273	298	273	298	273	298	273	298	Ref.
1-mim	14.6	10.6	119.4	76.3	92.4	64.9	101.0	79.9	NA	NA	102.9	96.87	7*b*
1-eim	19.3	11.5	117.8	73.7	87.3	61.3	99.3	75.4	NA	NA	97.4	86.6	7*b*
FJI-C1	NA	9.7	135.9	93.8	85.2	64.0	123.6	87.4	NA	NA	160.9	141.	20
FJI-C4	32.7	18.4	82.8	72.5	70.1	61.4	73.4	66.3	NA	NA	74.7	71.5	18
UTSA-33a	23.6	12.9	112.0	83.6	84.5	60.9	77.6	61.9	NA	NA	NA	NA	17*a*
UTSA-34a	26.1	14.7	103.6	80.3	78.1	58.9	72.35	62.4	NA	NA	NA	NA	17*b*
BUT-70A	16.1	9.7	93.8	69.5	53.0	36.9	62.7	42.7	72.1	57.4	69.4	53.0	21*b*
BUT-70B	14.3	9.6	120.5	87.1	94.2	49.0	68.9	53.3	76.7	69.8	69.3	64.5	21*b*
SBMOF-1	22.2	18.3	30.1	28.9	26.5	29.0	26.6	28.8	NA	NA	NA	NA	21*a*
SBMOF-2	27.5	17.5	73.2	64.5	68.2	59.4	68.8	62.1	58.3	64.8	58.1	64.9	21*a*
UPC-21	43.2	25.7	196.5	139.5	123.1	98.4	137.6	104.3	124.1	110.1	116.2	103.0	19
UPC-32	31.3	18.9	85.0	60.6	74.1	57.2	80.2	66.1	110.1	98.2	104.3	84.9	10*d*
UPC-33	9.7	7.0	65.1	44.3	43.6	31.1	51.8	35.0	114.2	94.3	111.8	93.6	10*b*
UPC-35	11.0	4.8	72.5	44.4	56.4	35.9	70.1	40.9	138.1	118.3	128.7	111.3	This work

pore sizes of **UPC-35**, which match well with the kinetic diameters of C_3 light hydrocarbons. Meanwhile, the selectivities of C_3H_6 to C_2H_2, C_2H_4 and C_2H_6 are 4.8, 7.5 and 5.3 at 1 bar and 273 K, respectively. These values approximate the selectivities of C_3H_6 with respect to C_2H_2, C_2H_4 and C_2H_6 as 4.9, 6.9 and 5.5 at 1 bar and 298 K, meaning that **UPC-35** can also selectively adsorb C_3H_6 from C_2 hydrocarbons at room temperature (Fig. 3d, 3e, and 3f and Table S7, ESI†).

In conclusion, by utilizing the solvent regulation approach, we have developed and characterized a pair of framework-interpenetration isomers (**UPC-34** and **UPC-35**) based on Cu-paddlewheel SBUs and a tripodal ligand with C_2 symmetry. The interpenetrated framework (**UPC-35**) is more stable than the non-interpenetrated one (**UPC-34**). **UPC-35** has the right pore size to maximize interactions between the gas and the framework, so it exerts a high separation selectivity for C_3 light hydrocarbons relative to CH_4 (159.5 and 121.6 for C_3H_6/CH_4 and C_3H_8/CH_4 at 273k and 1 bar) and can selectively adsorb C_3H_6 from C_2 hydrocarbons. These results indicate that **UPC-35** will be a promising candidate for light hydrocarbon separation in the near future (Table 1).

Conflicts of interest

The authors declare no competing financial interest.

Acknowledgements

This work was supported by the NSF of China (Grant No. 21571187, 21771191, and 21571137), Taishan Scholar Foundation (ts201511019), the Shandong Natural Science Fund (ZR2017QB012), the Fundamental Research Funds for the Central Universities (14CX02213A and 16CX05015A), the Foundation of State Key Laboratory of Structural Chemistry (20160006), and the Applied Basic Research Projects of Qingdao (16-5-1-95-jch).

Notes and references

1 H. W. Haring, *Industrial Gases Processing*, Wiley-VCH, 2008.
2 S. Matar and L. F. Hatch, *Chemistry of Petrochemical Processes*, Gulf Publishing Company, 2nd edn, 2000.
3 T. Ren, M. Patel and K. Blok, *Energy*, 2006, **31**, 425–451.
4 (*a*) H. R. Himmen and H. J. Reinhardt, *Chem. Eng.*, 2009, **116**, 48–53; (*b*) D. J. Safarik and R. B. Eldridge, *Ind. Eng. Chem. Res.*, 1998, **37**, 2571–2581.
5 L. Li, X. S. Wang and J. Liang, *ACS Appl. Mater. Interfaces*, 2016, **8**, 9777–9781.
6 (*a*) S. Aguado, G. Bergeret and C. Daniel, *J. Am. Chem. Soc.*, 2012, **134**, 14635–14637; (*b*) L. B. Li, R. B. Lin and R. Krishna, *J. Am. Chem. Soc.*, 2017, **139**, 7733–7736.
7 (*a*) Y. B. Zhang;, H. Furukawa and N. Ko, *J. Am. Chem. Soc.*, 2015, **137**, 2641–2650; (*b*) H. R. Fu and J. Zhang, *Inorg. Chem.*, 2016, **55**, 3928–3932; (*c*) A. H. Assen, Y. Belmabkhout and K. Adil, *Angew. Chem., Int. Ed.*, 2015, **54**, 14353–14358.
8 (*a*) J. Li, H. R. Fu and J. Zhang, *Inorg. Chem.*, 2015, **54**, 3093–3095; (*b*) W. Lu, Z. Wei and Z. Y. Gu, *Chem. Soc. Rev.*, 2014, **43**, 5561–5593.
9 (*a*) H. R. Fu and J. Zhang, *Chem. – Eur. J.*, 2015, **21**, 5700–5703; (*b*) D. S. Zhang, Z. Chang and Y. F. Li, *Sci. Rep.*, 2013, **3**, 3312; (*c*) N. Sikdar, S. Bonakala and R. Haldar, *Chem. – Eur. J.*, 2016, **22**, 6059–6070; (*d*) X. Y. Li, Y. Z. Li and Z. Zhu, *Chem. Commun.*, 2017, **53**, 12970–12973; (*e*) Y. Z. Li, H. H. Wang and Z. Zhu, *Chem. – Eur. J.*, 2018, **24**, 865–871; (*f*) L. G. Ding, B. J. Yao and Y. B. Dong, *Inorg. Chem.*, 2017, **56**, 2337–2344.
10 (*a*) H. Furukawa, K. E. Cordova and M. O'Keeffe, *Science*, 2013, **431**, 123044; (*b*) W. D. Fan, Y. T. Wang and Q. Zhang, *Chem. – Eur. J.*, 2017, **23**, 1–8; (*c*) Y. Y. Yang, Z. J. Lin and T. T. Liu, *CrystEngComm*, 2015, **17**, 1381–1388; (*d*) S. K. Elsaidi, M. H. Mohamed and L. Wojtas, *J. Am. Chem. Soc.*, 2014, **136**, 5072–5077; (*e*) W. D. Fan, Y. T. Wang and Z. Y. Xiao, *Chin. Chem. Lett.*, 2018, **29**, 865–868.

11 A. Cadiau, K. Adil and M. Eddaoudi, *Science*, 2016, **353**, 137–140.
12 P. Q. Liao, W. X. Zhang and J. P. Zhang, *Nat. Commun.*, 2015, **6**, 8697.
13 Z. Zhang, S. Xiang and B. L. Chen, *Inorg. Chem.*, 2012, **51**, 4947–4953.
14 (*a*) Z. J. Zhang, S. C. Xiang and Y. S. Chen, *Inorg. Chem.*, 2010, **49**, 8444–8448; (*b*) T. L. Hu, H. L. Wang and B. Li, *Nat. Commun.*, 2015, **6**, 7328.
15 (*a*) H. L. Jiang, T. A. Makal and H. C. Zhou, *Coord. Chem. Rev.*, 2013, **257**, 2232–2249; (*b*) M. Bosch, S. Yuan and W. Rutledge, *Acc. Chem. Res.*, 2017, **50**, 857–865.
16 (*a*) Q. G. Zhai, X. H. Bu and X. Zhao, *Acc. Chem. Res.*, 2017, **50**, 407–417; (*b*) K. Adil, Y. Belmabkhout and R. S. Pillai, *Chem. Soc. Rev.*, 2017, **46**, 3402–3430; (*c*) D. M. Chen, J. Y. Tian and C. S. Liu, *Chem. Commun.*, 2016, **52**, 8413–8416.
17 (*a*) Y. B. He, Z. J. Zhang and S. C. Xiang, *Chem. Commun.*, 2012, **48**, 6493–6495; (*b*) Y. B. He, Z. J. Zhang and S. C. Xiang, *Chem. – Eur. J.*, 2012, **18**, 613–619.
18 L. Li, X. S. Wang and J. Liang, *ACS Appl. Mater. Interfaces*, 2016, **8**, 9777–9781.
19 M. H. Zhang, X. L. Xin and Z. Y. Xiao, *J. Mater. Chem. A*, 2017, **5**, 1168–1175.
20 Y. B. Huang, Z. J. Lin and H. R. Fu, *ChemSusChem.*, 2014, **7**, 2647–2653.
21 (*a*) A. M. Plonka, X. Y. Chen and J. B. Parise, *Chem. Mater.*, 2016, **28**, 1636–1646; (*b*) Z. J. Guo, J. Yu and Y. Z. Zhang, *Inorg. Chem.*, 2017, **56**, 2188–2197.